Experimental verification of surface plasmon amplification on a metallic transmission grating

D. J. Park, S. B. Choi, K. J. Ahn, and D. S. Kim*
Department of Physics and Astronomy, Seoul National University, Seoul 151-742, Korea

J. H. Kang and Q-Han Park
Department of Physics, Korea University, Seoul 136-701, Korea

M. S. Jeong and D.-K. Ko
Advanced Photonic Research Institute, Gwangju Institute of Science and Technology, 500-712 Gwangju, Korea
(Received 4 October 2007; revised manuscript received 4 February 2008; published 27 March 2008)

We report on a near-field amplification in a transmission metallic grating, whereby the spatially and spectrally resolved near-field intensity reaches ~20 times the incident intensity at the surface plasmon polariton resonance. The amplified value is maintained up to ~2 μm away from the surface. Our experiments show that the near-field amplification in the transmission grating, which is strongly implied in a recent superlens design, indeed occurs at the surface plasmon polariton resonance. Theoretical calculation shows good agreement with experiment and also reveals that the horizontal magnetic field is predominantly amplified. Our results suggest that a grating-assisted superlens should have its optimal functional wavelength right around the surface plasmon resonance.

DOI: 10.1103/PhysRevB.77.115451 PACS number(s): 73.20.Mf, 71.45.Gm, 24.10.Ht, 79.60.Jv

Many intriguing properties of metallic diffraction gratings involve excitation of surface waves. For instance, Wood's anomaly[1–3] originates from the energy loss experienced by the incoming light when the energy-momentum condition is met for creating the surface plasmon polaritons on the grating surface. In the past decade, the surface plasmon enhanced transmission in two-dimensional and one-dimensional gratings has been a topic of intense research interest,[4–14] both from experimental and theoretical points of view. Recently, the one-dimensional diffraction grating has become a centerpiece in superlens imaging[15,16] since the resonantly excited surface plasmon polaritons (SPPs) on the grating surface are expected to supply an amplified near field, which is the most essential factor in superlensing.[17–23]

Even though many theoretical works and far-field experiments[24–26] suggest huge near-field *amplification*, it is necessary to confirm this by direct measurement of the near field for the far-field intensity does not determine the near-field intensity which contains various evanescent field components that do not propagate into the far field. Figure 1 shows three possible examples of the near-field intensity, when the far-field transmission is kept very small. The black curve describes the case where the incident light experiences no amplification around the slit. In the second case depicted in the red curve, the near-field intensity may exceed 1, but the amplification is so small that it renders the grating essentially useless. The third case is the most desirable case for superlensing, depicted in the green curve; dramatic amplification much larger than incident intensity is manifested.

In this paper, we describe the results of performing near-field spectroscopy using a broadband femtosecond Ti:sapphire laser with wavelength range from 740 to 840 nm. Normalized near-field intensity is taken by comparing with the bare-sapphire spectrum taken by the same method. We found that at the maximum, the near-field intensity is about 20 times larger than the incident intensity, which occurs at the SPP resonance. The decay profile measured by varying the tip to sample demonstrates that the amplified intensity is maintained up to the relatively large distance of about 2 μm. Spectrally and spatially resolved intensity profiles reveal that the periodicity-assisted constructive interference of the counterpropagating surface plasmon waves is the major source of such large near-field amplification. Theoretical considerations with partial wave expansion[2] combined with surface impedance boundary condition[27] (SIBC) suggest that the major amplified field component is the horizontal magnetic field.

A metallic transmission grating with thickness $t=78$ nm, period $d=761$ nm, and grating opening $a=100$ nm is prepared by electron beam lithography on a gold film thermally evaporated on a sapphire substrate. Figure 2(a) shows the experimental schematic. An x-polarized femtosecond Ti:sapphire laser centered at 780 nm having 30 nm full width at half maximum is normally incident upon the substrate side of the grating and collected by a metal-coated near-field scanning optical microscope (NSOM) probe sitting on the slit opening. The near-field spectrum $I_{near}(\lambda)$ is then resolved by a monochromator and a charge-coupled device camera,

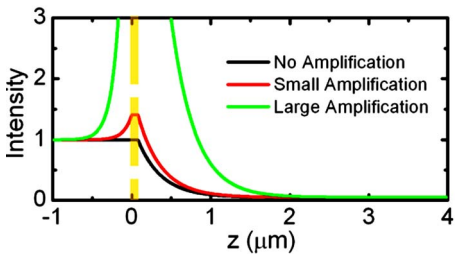

FIG. 1. (Color online) Schematic diagram of various near-field intensities which result in the same far-field transmittance. Black curve indicates no amplification, red curve indicates small amplification, and green curve indicates large amplification of the near field.

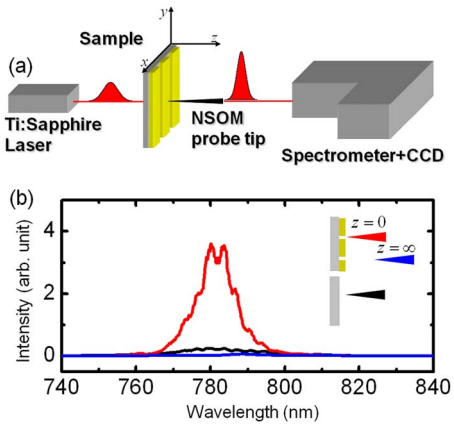

FIG. 2. (Color online) (a) Schematic of experimental setup, also with coordinates. (b) Measured spectra for 740 to 840 nm for reference (black curve), near field at slit opening region $x=0$ (red curve), and far field (blue curve).

which is compared with the reference spectrum $I_{ref}(\lambda)$ measured through the bare sapphire substrate. Strikingly, the near-field intensity shown in Fig. 2(b) (red line) is 2 or 3 orders of magnitudes larger than the far-field transmitted intensity $I_{far}(\lambda)$ (blue line). At its peak, it is much stronger even than the incident intensity.

Normalized near-field and far-field intensities are obtained by dividing the signal with a reference: $T_{near}=I_{near}/I_{ref}$ and $T_{far}=I_{far}/I_{ref}$. While far-field intensity reproduces the conventionally measured transmittance, as shown in the blue curve in Fig. 3(a), remarkably the near-field intensity reaches the maximum value of ~20 at the resonant wavelength 783 nm. This resonance coincides almost exactly with the flatband SPP resonance with momentum $2\pi/d$: $\lambda_{sp}=d\sqrt{\varepsilon_m/(1+\varepsilon_m)}=778$ nm, where ε_m denotes the gold dielectric function.[28] This strongly implies that SPP makes a dominant contribution in near-field amplification.

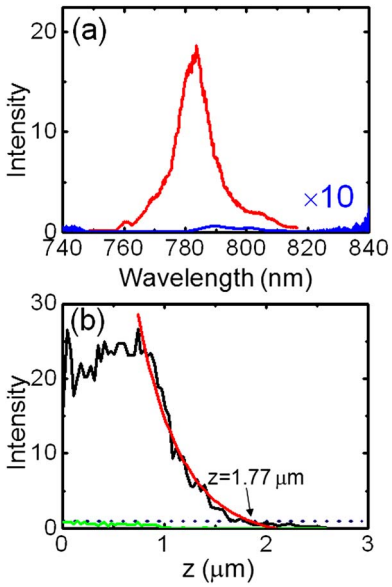

FIG. 3. (Color online) (a) Normalized near-field (red curve) and far-field (blue curve) spectra. (b) Decay profile along the z direction for $\lambda=783$ nm (black curve) and $\lambda=810$ nm (blue curve), also with linear fitting at exponential decay region (red line).

Dependency along the z direction shows a more dramatic feature of the near-field amplification. The black curve in Fig. 3(b) denotes the z-dependent decay profile at the SPP resonance, and the blue curve shows the decay at an off-resonant wavelength $\lambda=810$ nm. In off-resonance [green curve in Fig. 3(b)], intensity never exceeds 1 [dotted line in Fig. 3(b)] even in the near-field region and shows monotonic decay, referred to as "no amplification" in Fig. 1. On the other hand in SPP resonance, the field intensity shows strong amplification and even a slight increase with increasing z to reach ~30 at $z\sim0.8$ μm and then an evanescent decay. In the decay region, an exponential fitting has been made (red curve) to a give a decay length of 413 nm, which is reasonably matched with the calculated value of 297 nm $=\lambda/4\pi/\sqrt{\lambda^2/d^2-1}$. The most likely source of the error is a slight deviation $\theta\sim1°$ from the nominally normal incidence of the incoming light, which would introduce an effective d of about 774 nm $\sim d(1+\theta)$.

The amplified intensity of larger than unity is maintained until $z=1.77$ μm. This situation is described in Fig. 1 as a case of "large amplification," where the amplified intensity is delivered beyond the subwavelength region. In the superlens imaging described in Ref. 15, the near-field intensity needs to be as large as possible, and the imaging plane needs to be as far away from the object plane as practically possible. While our results show that the grating structure used in Ref. 15 is a very plausible solution to achieve superlensing, the experimentally observed initial slight increase with z needs further discussion. We believe that it is related to the image dipole effect, which introduces a component which *decreases* as the tip approaches the near field.[29–31] Our calculated result taking the full tip shape into consideration is in qualitative agreement with experimental results.[32]

Strong wavelength dependence of near-field amplification implies that certain wave vectors are selectively amplified. The spatially resolved near-field pattern is shown in Fig. 4(a). The measurement is performed in the following way: The near-field probe picks up the spectrum at $x=0$, and then it moves to another position $x=0+n\Delta$ where $\Delta=50$ nm, and picks up the spectrum again. The nice standing wave pattern whose period is exactly half of the grating period is observed at resonance, and then rapidly dies out as the wavelength deviates from resonance. This standing wave pattern comes from constructive interference between propagating and counterpropagating waves which are bound to the surface. To be constructive, the wave vectors of these waves should match the crystal momentum of $G=2\pi/d=8.256\times10^4$ cm^{-1}. The fact that the experimental resonance occurs at 783 nm while the SPP wavelength having the momentum G is 778 nm demonstrates that resonant excitation of SPP waves in the grating is responsible for the large enhancement.

A cross-sectional plot along the x direction at the SPP resonance, which is depicted in Fig. 4(b), shows a high visibility of the SPP wave at ~0.734 μm. This indicates that the first order diffraction terms which couples to the SPP wave dominate above all other terms. To understand our experiments, we perform a Rayleigh partial wave expansion calcu-

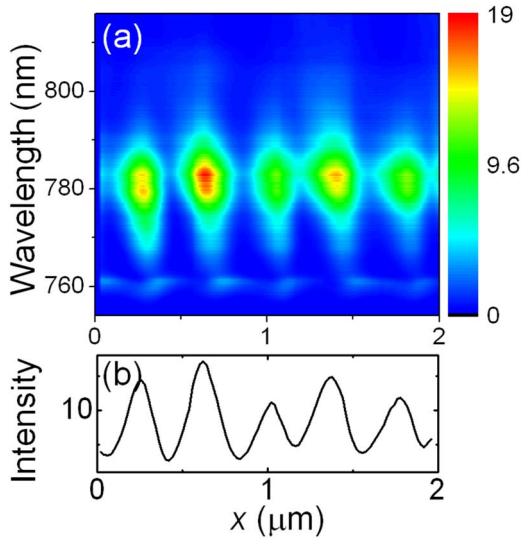

FIG. 4. (Color online) (a) Near-field intensity as a function of wavelength (λ) and position (x). (b) Cross-sectional plot along the x direction at SPP resonance λ=783 nm.

lation of the horizontal magnetic field H_y,[2,12,27]

$$H_y = \sum_n [H_n \cos(k_{nx}x - \omega t)e^{-\kappa_n z}], \tag{1}$$

where n is an integer and $k_{nx}=2\pi n/d$ and $\kappa_n=\sqrt{k_{nx}^2-k_o^2}$ denote the wave vector components along the x direction and z direction for each diffraction order, respectively. Cavity mode expansion is also considered in the slit opening region. Boundary matching is separately considered on the metal surface and slit opening region: conventional continuity of the field in the slit opening region and SIBC on the metal surface. SIBC connects the electric and magnetic fields as $E_x=Z\hat{n}\times H_y$, where $Z=1/\sqrt{1+\varepsilon_m}$. Solving coupled equations taken from these boundary matchings give Fourier amplitude for each diffraction order. Near resonance, it is easy to show that only the ±1 diffraction orders contribute

$$T_1 = C\frac{\frac{1}{d}\int u(x)dx}{\frac{\eta}{2\pi i}(1-e^{i(2\pi/d)x})} + C\frac{\frac{1}{d}\int u(x)e^{-i(2\pi/d)}dx}{i\sqrt{k_o^2-\frac{2\pi}{d}}-\frac{(d-a)\eta}{d}}, \tag{2}$$

where $\eta=Zk_0/i$, d is the period, a is the slitwidth, $u(x)$ is the cavity mode wave function inside the slit, and C is a thickness-related term giving rise to the Fabry–Pérot effect inside the slit cavity.[11,12,33] The second term in the right hand side of the equation has a pole when

$$\lambda = d\sqrt{1-\frac{(d-a)^2}{d^2}\frac{1}{1+\varepsilon_m}}. \tag{3}$$

This wavelength is very close to the SPP resonance wavelength of $\lambda=d\sqrt{\varepsilon_m/(1+\varepsilon_m)}$ for small a and explains why we observe large amplification near the SPP resonance. The large *near-field amplification* is theoretically reconstructed, keeping all orders, as depicted in the black curve in Fig. 5. This calculation reproduces a strong peak at the SPP resonance and supports our claim that SPP excitation is the major source of near-field amplification.

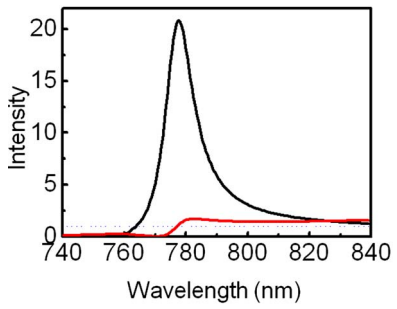

FIG. 5. (Color online) Calculated spectrum of horizontal magnetic field H_y (black curve) and horizontal electric field E_x (red curve). Blue dotted line denotes unity.

Applying the Helmholtz equation on the H_y component gives the horizontal electric field component E_x,

$$E_x = -\frac{1}{ik_0}\sum_n [H_n\kappa_n \cos(k_{nx}x - \omega t)e^{-\kappa_n z}]. \tag{4}$$

The spectrum with this calculation is depicted by the red curve in Fig. 5. Contrary to the H_y component, E_x shows no significant amplification. These results indicate that the horizontal magnetic field is amplified due to SPP generation. This amplified magnetic field is measured by an apertured NSOM probe.[34,35]

Before closing theoretical considerations, we want to mention the other electromagnetic component E_z. Actually, this component is not detectable with the apertured NSOM probe since electric or magnetic dipoles induced on top of the tip apex do not couple to the z component due to probe geometry. However, if we apply the Helmholtz equation again to the magnetic field, we can get the E_z component as follows:

$$E_z = -\frac{1}{ik_0}\sum_n [H_n k_{xn} \sin(k_{nx}x - \omega t)e^{-\kappa_n z}]. \tag{5}$$

Since k_x and k_0 are quite similar to each other at $\lambda\sim\lambda_{SPP}$, we can expect that the E_z component is of the same strength and of the same shape as H_y, except for the 90° phase shift. This implies that we would expect the vertical electric field to be amplified with almost the same magnitude as the horizontal magnetic component.

In conclusion, we have made a fully quantitative description of the near-field amplification in the transmission grating. The measured near-field amplification reaches 20 at its maximum and shows an amplified value until 1.77 μm along the direction normal to the surface. Spatially and spectrally resolved near-field profiles reveal that the resonantly excited SPP waves explain this amplification. Theoretical considerations show very good agreement with experiment and strongly suggest that the main amplified electromagnetic field that we observe is the horizontal magnetic field. Our results indicate that the transmission grating is the key component of the superlens, as a near-field resonant amplifier.

Financial support of the work in Korea by the Korean Government (MOST, MOEHRD) through KRF (Grants No. C00012 and No. C00032), by KOSEF, by SEOUL R&D programs, and by the Nano R&D program (Grant No. 2007-02939) is gratefully acknowledged. The authors are grateful to Christoph Lienau, Claus Ropers, and Joong Wook Lee for many valuable discussions and also to Minah Seo for discussions and art works for the figures.

*Corresponding author: dsk@phya.snu.ac.kr

[1] R. W. Wood, Proc. Phys. Soc. London **18**, 269 (1902).
[2] L. Rayleigh, Proc. Phys. Soc. London A **79**, 399 (1907).
[3] R. W. Wood, Phys. Rev. **48**, 928 (1935).
[4] Q. Cao and P. Lalanne, Phys. Rev. Lett. **88**, 057403 (2002).
[5] S. I. Bozhevolnyi, J. Erland, K. Leosson, P. M. W. Skovgaard, and J. M. Hvan, Phys. Rev. Lett. **86**, 3008 (2001).
[6] I. R. Hooper and J. R. Sambles, Phys. Rev. B **65**, 165432 (2002).
[7] W. L. Barnes, W. A. Murray, J. Dintinger, E. Devaux, and T. W. Ebbesen, Phys. Rev. Lett. **92**, 107401 (2004).
[8] S. C. Hohng *et al.*, J. Korean Phys. Soc. **46**, s205 (2005).
[9] S. C. Hohng *et al.*, Appl. Phys. Lett. **81**, 3239 (2002).
[10] D. S. Kim *et al.*, Phys. Rev. Lett. **91**, 143901 (2003).
[11] J. W. Lee, M. A. Seo, D. S. Kim, S. C. Jeoung, C. Lienau, J. H. Kang, and Q. H. Park, Appl. Phys. Lett. **88**, 071114 (2006).
[12] K. G. Lee and Q. H. Park, Phys. Rev. Lett. **95**, 103902 (2005).
[13] L. Martin-Moreno, F. J. Garcia-Vidal, H. J. Lezec, K. M. Pellerin, T. Thio, J. B. Pendry, and T. W. Ebbesen, Phys. Rev. Lett. **86**, 1114 (2001).
[14] C. Ropers, D. J. Park, G. Stibenz, G. Steinmeyer, J. Kim, D. S. Kim, and C. Lienau, Phys. Rev. Lett. **94**, 113901 (2005).
[15] Z. Liu, S. Durant, H. Lee, Y. Pikus, N. Fang, Y. Xiong, C. Sun, and X. Zhang, Nano Lett. **7**, 403 (2007).
[16] R. Moussa, S. Foteinopoulou, L. Zhang, G. Tuttle, K. Guven, E. Ozbay, and C. M. Soukoulis, Phys. Rev. B **71**, 085106 (2005).
[17] L. Novotny, *Principles of Nano-Optics* (Cambridge University Press, Cambridge, 2006), pp. 34 and 392.
[18] H. Raether, *Surface Plasmons on Smooth and Rough Surfaces and on Gratings* (Springer-Verlag, Berlin, 1988), pp. 4–7.
[19] R. Merlin, Appl. Phys. Lett. **84**, 1290 (2004).
[20] S. Astilean, P. Lalanne, and M. Palamaru, Opt. Commun. **175**, 265 (2000).
[21] M. W. Feise, P. J. Bevelacqua, and J. B. Schneider, Phys. Rev. B **66**, 035113 (2002).
[22] D. O. S. Melville and R. J. Blaikie, Physica B **394**, 197 (2007).
[23] J. B. Pendry, Phys. Rev. Lett. **85**, 3966 (2000).
[24] Z. Liu, N. Fang, T. J. Yen, and X. Zhang, Appl. Phys. Lett. **83**, 5184 (2003).
[25] K. L. Van Der Molen, K. J. Klein Koerkamp, S. Enoch, F. B. Segerink, N. F. Van Hulst, and L. Kuipers, Phys. Rev. B **72**, 045421 (2005).
[26] T. W. Ebbesen, H. J. Lezec, H. F. Ghaemi, T. Thio, and P. A. Wolff, Nature (London) **391**, 667 (1998).
[27] H. Lochbihler and R. Depine, Appl. Opt. **32**, 3459 (1993).
[28] P. B. Johnson and R. W. Christy, Phys. Rev. B **6**, 4370 (1972).
[29] Z. H. Kim and S. R. Leone, J. Phys. Chem. B **110**, 19804 (2006).
[30] M. B. Raschke and C. Lienau, Appl. Phys. Lett. **83**, 5089 (2003).
[31] B. Knoll and F. Keilmann, Opt. Commun. **182**, 321 (2000).
[32] K. J. Ahn (unpublished).
[33] J. E. Kihm, Y. C. Yoon, D. J. Park, Y. H. Ahn, C. Ropers, C. Lienau, J. Kim, Q. H. Park, and D. S. Kim, Phys. Rev. B **75**, 035414 (2007).
[34] L. Novotny, *Principles of Nano-Optics* (Cambridge University Press, Cambridge, 2006), pp. 188–192.
[35] H. A. Bethe, Phys. Rev. **66**, 163 (1944).